Journal of the Southeastern Association for Research in Astronomy, 5, 51-55, 2012 February 1

POLARIMETRY OF EPSILON AURIGAE: INITIAL OBSERVATIONS OF THE 2009-2011 ECLIPSE

John A. C. Burdette[1]
Department of Physics and Astonomy, East Tennessee State University
Johnson City, TN 37614

and

Gary D. Henson
Department of Physics and Astronomy, East Tennessee State University,
Johnson City, TN 37614

ABSTRACT

Epsilon Aurigae is an eclipsing binary system consisting of an F0 supergiant (200 $R_{\odot}$) and a cool, opaque edge-on disk (2000 $R_{\odot}$) possibly encompassing a second star. V-band polarimetry data for Epsilon Aurigae's 2009-2011 eclipse is being obtained to better understand the system's geometry and the nature of its two components. Several polarized and non-polarized standard stars are also being observed in order to characterize the instrumental polarization and sources of measurement error in the polarimeter configuration and the measurement procedures for observations. We report here on the status of these observations at the midpoint of the eclipse and include a preliminary analysis of noise and instrumental effects in the measurements.
Subject headings: Polarization — Stars: eclipsing binaries — Methods: observational — Techniques: polarimetry

1. INTRODUCTION

Epsilon Aurigae is an eclipsing binary system consisting of an F0 supergiant and a cool, opaque edge-on disk. The supergiant is known to pulsate and the disk may be protoplanetary matter encompassing a protostellar object making Epsilon Aurigae a unique candidate for inquiry. The system's orbital period is 27 years with a primary eclipse duration of approximately 2 years. During the primary eclipse, the disk passes in front of the supergiant creating a flat-bottomed partial eclipse. This provides a unique opportunity to obtain information about the disk as it occults the supergiant. An international campaign is underway to observe the current eclipse which began in fall 2009 and will continue through early 2011 (see http://www.hposoft.com/Campaign09.html for details). We are contributing polarized light observations and their interpretation to this campaign. Polarized light from the limb of the supergiant is presumed to be the dominant source of polarization intrinsic to the system. Both non-radial pulsations in the supergiant and the partial eclipse create asymmetries leading to a net polarization. Observations of variations in this polarization will contain clues to characterizing the geometry of the disk and the supergiant's pulsations (Kemp et al. 1986, Henson 1989).

For polarized light measurements, linear polarization describes a constant angle of electric field orientation while circular polarization describes an electric field that rotates as it propagates. Polarized light is described by the four Stoke's parameters I, Q, U, and V which measure intensities of light and its polarized components. Using the equatorial reference frame, the I value describes total intensity, Q describes differences between North-South ($+Q$) and East-West ($-Q$) linearly polarized intensities, U describes differences between linearly polarized intensities oriented at $+/-45°$ ($+/-U$ respectively) from North-South, and V describes the differences between right and left circular intensities. Only linear polarization measurements (Q and U) were collected here.

Electronic address: burdettj@etsu.edu; hensong@mail.etsu.edu
[1] Southeastern Association for Research in Astronomy (SARA) NSF-REU Summer Intern

2. OBSERVATIONS

A polarimeter is attached to the 14-inch Schmidt-Cassegrain telescope at East Tennessee State University's Powell Observatory to collect data from polarized sources. The configuration is such that the polarized components of light collected by the telescope are reoriented by a rotatable half-wave plate and are then split into orthogonally polarized components by a Wollaston prism serving as an analyzer. A CCD camera then images the two beams, known as the ordinary and extraordinary rays ($o - ray$ and $e - ray$ respectively). The configuration of the polarimeter is illustrated in Figure 1.

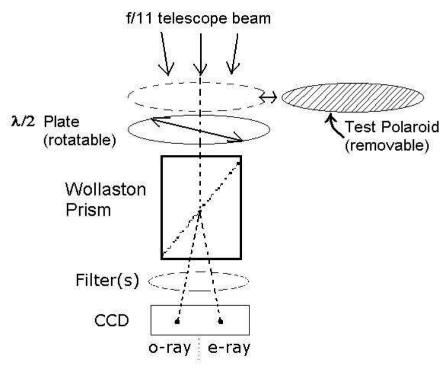

Fig. 1.— Polarimeter schematic taken from Hall & and Henson (2010).

A single data point consists of sixteen images differentiated by 22.5° rotations of the half-wave plate. Though only 90° of rotation (four images) are necessary to obtain $+/-Q$ and $+/-U$ values, the half-wave plate is rotated for 360 ° and all data for the complete rotation are averaged in order to minimize instrumental effects and error due to imperfections in the half-wave plate and/or prism orientation relative to incident light. A more detailed description of the polarimeter configuration and measurement procedure can be found in Hall & Henson (2010).

2.1. *Epsilon Aurigae Polarimetry*

The polarimetry data for Epsilon Aurigae presented here were collected from fall 2009 to early summer 2010. Typical exposure times for a single waveplate position ranged from 10 to 20 seconds, though longer exposures were taken for the last few observations. A set of 8 to 16 data points, each consisting of 16 images, was used to calculate the final normalized Q and U values for each night. For all images, bias, dark, and flat fields were applied using MIRA software. MIRA was then used to perform aperture photometry in order to determine net counts for the $o-ray$ and $e-ray$ image in each CCD frame. The intensity difference between the $o-ray$ and $e-ray$ was used to calculate $+/-Q$ and $+/-U$ values, which were in turn used to determine net Q and U values. The net linear polarization of light, P, was then calculated from net Q and U. For one 16-image data point, the calculations are outlined below.

First, a corrective term was calculated to account for asymmetries in the optical paths of the $o-ray$ and $e-ray$ (Equation (1)). Here, I_o represents intensity of the $o-ray$, I_e represents intensity of the $e-ray$, and subscript numbers represent the image number in the half-wave plate rotation sequence.

$$C_1 = \left[\frac{I_{o1}}{I_{e3}} \times \frac{I_{o3}}{I_{e1}} \times \frac{I_{o2}}{I_{e4}} \times \frac{I_{o4}}{I_{e2}}\right]^{\frac{1}{4}} \tag{1}$$

Additional corrective terms are calculated similarly where each subsequent C value depends upon the next four $o-ray$ and $e-ray$ intensities. This corrective term was then used in conjunction with the intensity ratios to determine a fractional polarization value for each image as shown below:

$$P_1 = \left[\frac{1 - C_1\left(\frac{I_{e1}}{I_{o1}}\right)}{1 + C_1\left(\frac{I_{e1}}{I_{o1}}\right)}\right] \tag{2}$$

For each group of 16 images, Q and U values were calculated by summing the appropriate fractional polarization values from Equation (2). These Q and U values were then used to determine polarization as outlined in Equations (3), (4,) and (5) below:

$$Q_{net} = \frac{\sum_{n=1}^{4}[P_{4n-3} - P_{4n-1}]}{8} \tag{3}$$

$$U_{net} = \frac{\sum_{n=1}^{4}[P_{4n} - P_{4n-2}]}{8}. \tag{4}$$

$$P_{net} = \sqrt{Q_{net}^2 + U_{net}^2} \tag{5}$$

The outline above is shown to indicate the dependence of final polarization values on the intensities of star images on the CCD. Thus, the precision of $o-ray$ and $e-ray$ intensities limits the precision of the fractional polarization calculation, and the signal-to-noise ratio (S/N) for the polarized flux is further limited by the small fractional polarization of incident light. A more complete description for every step in the calculations can be found in Hall & Henson (2010).

The set of V-band fractional polarization measurements for Epsilon Aurigae spanning fall 2009 to summer 2010 is illustrated in Figure 2. For these measurements, typical uncertainties per nightly point are on the order of 0.001 fractional polarization or 0.1%. The uncertainty shown here is the standard deviation among the set of 8 to 16 data points acquired each night. The total linear polarization, P, is shown in the top curve with the individual, normalized Q and U Stokes parameters plotted below. We have chosen not to display the polarization position angle in this figure since following the changes in Q and U provide more insight to the eclipse geometry. In addition, there is a known interstellar component closely aligned with the U parameter which dominates the mean level of polarization (Kemp et al. 1986). We have not removed this component from the data shown here. Approximate dates for the start of the ingress and full eclipse phases are shown at the bottom of the U parameter curve. Visual inspection of these curves shows long period, small amplitude variations in both the Q and U parameters. Such variability is known to arise from pulsations in the F0 supergiant which dominate the polarization curves both in and out of eclipse (Henson 1989). We see no obvious evidence of any major changes in the curves as the eclipse is progressing. It is possible the polarization changes from the supergiant pulsations are masking eclipse effects.

For this paper, we are only presenting these initial polarization curves in a simple qualitative manner. Observations of Epsilon Aurigae are continuing through the entire eclipse time interval and beyond. A more detailed analysis will be presented once data for the entire eclipse and for sufficiently establishing the pulsation behavior are obtained. Because variations in the polarization are small, the amount of observational uncertainty must be minimized in order to better interpret and model the observed changes. The measurement error shown in Figure 2 is larger than desired, but also larger than expected for the polarimeter instrument. We address this issue in the following section.

3. SOURCES OF MEASUREMENT ERROR

The polarimeter was installed during summer 2008, but modifications were required and the alignment of the optical arrangement was refined that fall. Standard star measurements were obtained in the first months of operation, but were limited and incomplete (Hall & Henson 2010). Several bright unpolarized and strongly polarized standard stars are continually being observed to more precisely determine the instrumental polarization and the limit of precision for the polarized light measurements. In this paper we focus mainly on sources of error for a measurement. Because there are several op-

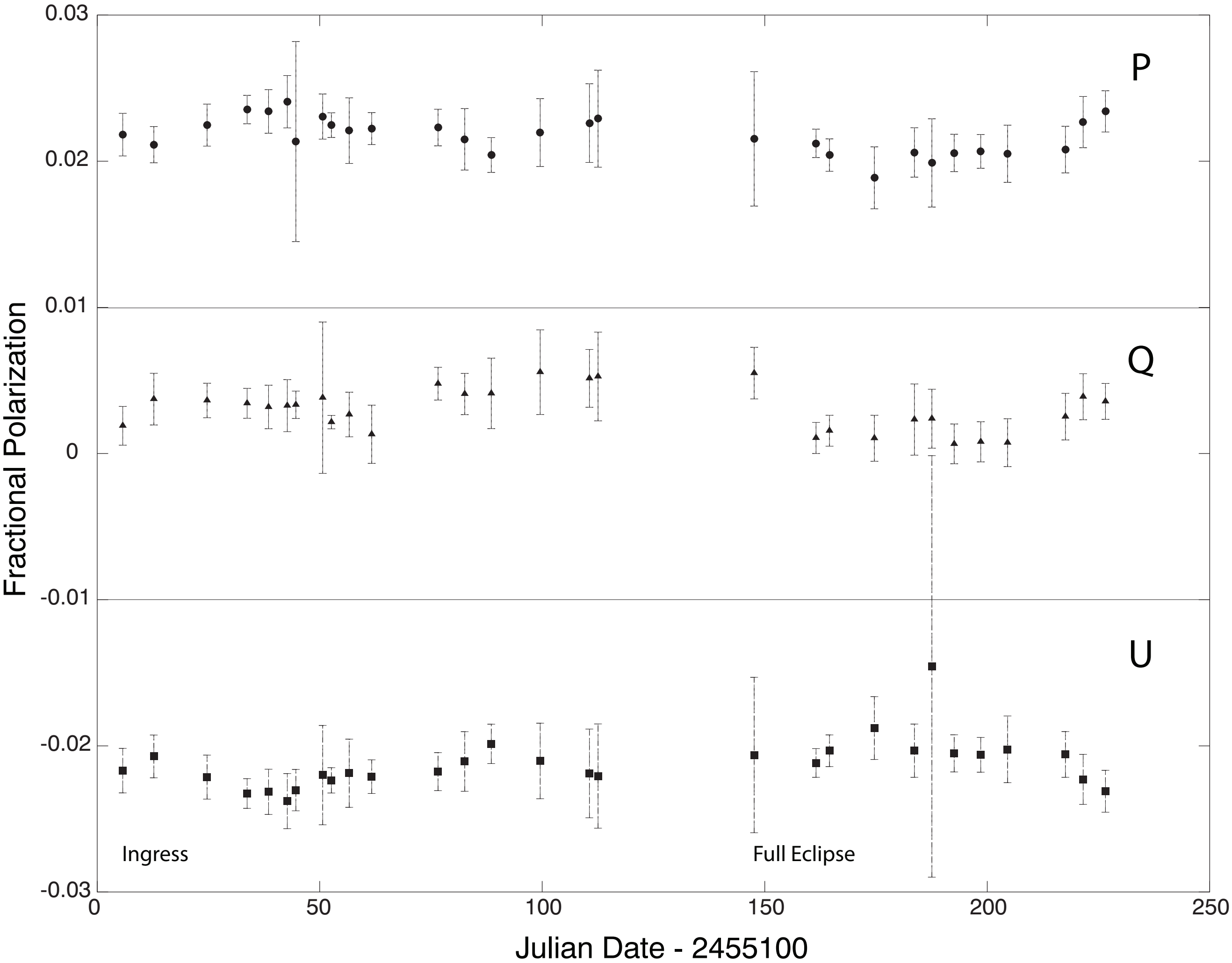

FIG. 2.— V band fractional polarization curves for Epsilon Aurigae. The approximate dates for eclipse ingress and for full eclipse are indicated at the bottom of the U parameter curve.

tical components involved in the polarimeter, it is easy for imperfections in their alignment and/or behavior to affect the incident light.

The standard stars were observed and the images reduced with a procedure identical to that used on Epsilon Aurigae. Exposure times varied due to intensity differences between objects, but in all cases the exposure time was chosen to obtain the maximum number of counts without saturating individual pixels. This was necessary to obtain the highest S/N possible as required for the weak polarized light signals. Our measured values, the associated measurement errors, and the expected values for the corresponding objects are reported in Table 1. Included in this table are measurements performed by Hall & Henson (2010) in late 2008 and early 2009 for comparison.

The measurements show that a small level of instrumental polarization is present in agreement with Hall & Henson (2010). More importantly for this discussion, the magnitude of the error in these measurements for even the brightest objects is on the order of 0.1% or greater. We note particularly that for the two brightest stars, Vega and Arcturus, integration times were significantly increased for the 2010 measurements over the 2009 measurements. However, the average polarization values and measurement errors were very consistent between the two sets of observations indicating the smallest achievable error to be limited to the level of 0.1%.

For polarimetry observations of Epsilon Aurigae, measurement error on the order of 0.025% is desired. This level of precision is needed to resolve changes in the P value due to the supergiant's pulsations versus effects of the eclipse. With errors on the order of 0.1% it is difficult to distinguish between these two sources of polarization. As Figure 2 shows, the error in the measurement can equal or exceed the magnitude of the variability in the polarization. Thus, we are investigating whether the true errors in the measurements may be smaller than those presented here. If this is the case, more accurate conclusions may be drawn concerning the sources and the magnitudes of the variation in polarized light.

With an ideal optical configuration, photometric error depends only upon photon noise. The S/N for a single star image, i.e. either the $o-ray$ or $e-ray$, collected with an ideal optical configuration is given as:

$$S/N = \sqrt{N} \tag{6}$$

where N is the number of photons detected. However, since only a small fraction of these photons represent the polarization signal for each half-wave plate position, the

TABLE 1
V Band Standard Star Polarization

Star	Mag.	Accepted P_{net} (%)[a]	2009 Observed P_{net} (%)	2009 Nights Observed[b]	2010 Observed P_{net} (%)	2010 Nights Observed[b]
Altair	0.77	0	0.1±0.1	2	0.3±0.2	3
Arcturus	-0.04	0	0.1±0.1	3	0.2±0.1	4
Deneb	1.25	0	–	–	0.3±0.2	2
Vega	0.03	0	0.2±0.1	5	0.2±0.1	4
HD 154445	5.70	3.67±0.05	3.8±0.7	3	3.7±0.5	3
HD 187929	3.5-4.5	1.8	1.6±0.2	1	1.9±0.5	1

[a]Bright Stars are expected to have zero polarization, highly polarized standards taken from Gehrels(1974)
[b]See text for comments on average integration times for each star per night

S/N for the polarization is greatly reduced. Patat & Romaniello (2006) define the S/N for our rotating half-wave plate measurements as:

$$S/N = \frac{1}{\sqrt{n} \times E_p} \quad (7)$$

where n is the total number of half-wave plate position angles per data point and E_p is the desired precision of the measurement. Thus, to attain error on the order of .02% for 16 half-wave plate positions, a S/N of 1250 for each $o - ray$ or $e - ray$ image for each CCD frame is desired. Since our images are slightly defocused (see the vignetting discussion below), we were able to use longer integration times to increase the S/N above the benchmark of 1250. However, there was no noticeable improvement in the measurement error. The error remained on the order of 0.1% for the bright standard stars. Thus, the limiting factor does not appear to be photon noise.

Patat & Romaniello (2006) present a detailed error analysis for a similar polarimeter configuration. In that analysis, imperfections in the half-wave plate and Wollaston prism were shown to contribute measurement errors on the order of 0.05%. Contributions to error due to non-ideal optics can be placed into two categories: geometric asymmetry and imperfections in the optical behavior of an element.

An ideal polarimeter is oriented in such a manner that incident light travels through each optical component normal to its surface. If this is not the case, several issues arise. A tilted wave-plate will refract light, which in turn scatters off of the prism, imparting it with some polarization. A tilted prism will cause the $o - ray$ and $e - ray$ to follow optical paths of differing length, causing them to be incident on the CCD at differing angles. Since a CCD measures fewer counts as incident light strikes it at an angle, this can cause fewer counts to register for either ray. Although the polarimeter has been constructed to position all elements to have surfaces perpendicular to the light path, we are aware of vignetting issues due to the small diameter of our Wollaston prism. This may be a significant noise contribution since this vignetting causes focus issues. The two beams cannot achieve their best focus simultaneously, so we focus the two beams to obtain similar FWHM values.

Issues with the optical behavior of the elements can be described succinctly. An imperfect half-wave plate will not reorient polarized light perfectly. Thus, Q and U values may be slightly distorted as net counts for $+/-$Q and $+/-$U vary. An imperfect Wollaston prism will not split polarized light into components that are 100% orthogonal. Thus, the $o - ray$ and $e - ray$ will be slightly different, again distorting Q and U values. Such behaviors affect the efficiency of the polarimeter while introducing measurement error.

In addition to the above instrumental effects, Patat & Romaniello (2006) also describe how the nature of flat-fielding calibration was found to be problematic for polarimetry. Our common sky-source for flat-field images is the twilight sky. Sky light, however, is polarized, so flat-field measurements must account for this in some way. The half-wave plate alignment was initially optimized for the $+Q$ position. We took care to point the telescope toward the western horizon where sunlight was forward scattered to minimize polarization in flat-field images. Such a location above the setting sun should, in general, provide a neutral point in the skylight polarization (Lee 1998). However, during flat-field acquisitions, subtle intensity variations were seen between wave plate rotations. Thus, images from all 16 position angles were averaged to create a master Q and U flat with the intent of minimizing effects due to twilight sky polarization. The background sky conditions due to moonlight and light clouds during data collection also create a background sky polarization. This background polarization further decreases the S/N of the polarized light measurement.

4. CONCLUSIONS

Our initial polarized light observations of the current Epsilon Aurigae eclipse show variability at levels comparable to the 1984-1986 eclipse. However, we have not been able to clearly distinguish between eclipse effects and those caused by the pulsations in the supergiant in the data presented here. However, we note that these data cover only the period through mid-eclipse and the largest eclipse effect was observed during egress for the 1984-1986 eclipse (Kemp et al. 1986). We have confirmed that a small level of instrumental polarization is present for the instrument being used for the observations and that it appears to be constant over time. The measurement error has been found to be much larger than desired which could potentially limit the interpretation of the variability. We suspect that the flat-fielding calibration is the most likely source of the large measurement error and are continuing to explore other techniques such as the use of dome-flats. The goal is to obtain measurement errors on the order of 0.02% to better resolve the difference between the effects of the eclipse versus the supergiant pulsations in the polarized light from the system.

This project was funded by the National Science Foundation Research Experiences for Undergraduates (REU) program through grant NSF AST-1004872.

REFERENCES

Gehrels, T. 1974, Planets, Stars, and Nebulae studied with photopolarimetry (Tucson: The University of Arizona Press)

Hall, S. W. & Henson, G. D. 2010, JSARA, 4, 2

Henson, G. D., 1989, PhD dissertation, University of Oregon

Kemp, J. C., Henson, G. D., Kraus, D. J., Beardsley, I. S., Carroll, L. C., Ake, T. B., Simon, T., and Collins, G. W. 1986, AJ, 300, L11

Patat, F., & Romaniello, M. 2006, PASP, 118, 146

Lee, R. L. 1998, Applied Optics, 37, 1465